ELECTROMAGNETIC SCATTERING FROM TWO-DIMENSIONAL COMPOSITE OBJECTS

Ahmed A. Kishk and Paul M. Goggans
Department of Electrical Engineering
University of Mississippi
University, MS 38677

ABSTRACT. Different surface integral equations are presented for two-dimensional composite objects. The objects consist of impedance bodies partially coated with dielectric materials. In all of the formulations, the impedance boundary condition is applied on the impedance surface to reduce the matrix size in the numerical solution. The integral equations are reduced to a system of linear equations via the point matching technique. Application of the point matching technique is straight forward for two dimensional objects. Because of this surface discontinuities can be treated easily without the problems encountered when using triangle basis functions as a result, consideration of two-dimensional objects gives a clear picture of the accuracy that can be obtained using these formulations. Two of the formulations discussed herein overcome the problem of internal resonance. The numerical solutions are verified either by comparison with the analytical solutions for cylindrical objects or by applying self consistency tests for targets without analytical solutions.

1 INTRODUCTION

Recently, interest has been renewed in using the impedance boundary conditions (IBC) in the solution of electromagnetic scattering problems. Use of the IBC can simplify the solution of the many complex electromagnetic problems for which it is valid. However, composite objects of complex structure, in terms of both material type and geometry, are difficult to treat using the IBC because the IBC is often not valid on all object surfaces. Using the exact boundary conditions to solve these problems is uneconomical and requires complicated programming when compared to a method incorporating the IBC.

The IBC is a valid approximation under certain conditions [1-4]. The problem of extending the IBC for use on surfaces where use of the standard IBC would usually be considered questionable has been investigated to some extent. Generalized impedance boundary conditions were proposed in [5] and [6] for this purpose. Unfortunately, use of these generalized impedance boundary conditions comes at the expense of considerable analytical complications and requires specialized researchers to treat each new geometry.

An alternative to using generalized impedance boundary conditions is to use the usual IBC only on surfaces where it is valid. Since IBC is a localized approximation, it can be used on surfaces where it is valid and the exact boundary conditions can be used on the rest of the object [7]. In a practical sense, the IBC can be used for any surface type for which the surface impedance can be determined. In cases of rapid spatial variation of the surface impedance, knowledge of the derivative of the surface impedance is also required. In numerical solutions the surface impedance must be slowly varying to allow for proper piecewise approximation on the surface segmentation. The idea of using both the impedance boundary condition and the exact boundary conditions in a single formulation leads to a technique that is both accurate and efficient.

In this paper such a technique is implemented for two-dimensional (2D) scatterers. Here, four different surface integral formulations are implemented for two-dimensional problems. The method of moments using the point matching technique is then used to reduce the integral equations to matrix equations. The separation of the two transverse polarizations in the 2D problem and the ability to easily implement point matching in the numerical solution of the 2D problem (and so to treat surface discontinuities) will lead to a more complete understanding of the limitations imposed on this technique than is possible with three-dimensional implementations.

2 FORMULATION

Consider the general geometry of a two-dimensional scatterer consisting of an impedance body that is partially coated with dielectric as illustrated in Fig. 1. The impedance body has known surface impedance and the dielectric coating is linear, isotropic, and homogeneous. For this geometry, there are three distinct regions: V_2 constituting the impedance body, characterized by surface impedance η_c; V_0, the exterior of the scatterer, characterized by the permittivity and permeability of the free space (ϵ_0, μ_0); and

V_1, the dielectric region, characterized by the permittivity and permeability (ϵ_1, μ_1). The excitation is an

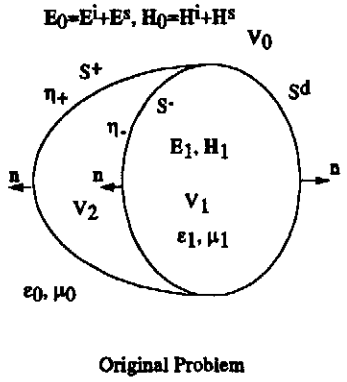

Fig. 1 Geometry of the Original Problem

electromagnetic plane wave of incident fields E^i and H^i. The total electric and magnetic fields in region V_v are denoted by E_v and H_v, respectively. In V_2 the total fields are not of interest and have therefore been assumed to be zero for convenience. The region V_1 is bounded by S^-, the boundary surface between V_1 and V_2, and S^d, the boundary surface between V_1 and V_0. The region V_0 is bounded by S^+, the boundary surface between V_0 and V_2 , and S^d. The normal unit vector $\hat{n}$ on the surface S^- points into the region V_2 and out of the region V_1. On the surfaces S^+ and S^d, $\hat{n}$ points into region V_0 and out of regions V_2 and V_1.

The equivalence principle is applied to create the two auxiliary problems shown in Fig. 2 [7]. The first (Fig. 2a) is the exterior equivalent problem that is electromagnetically equivalent to the original problem in region V_0. The second (Fig. 2b) is equivalent to the original problem in region V_1.

In the TM case the equivalent electric currents J^d, J^+, and

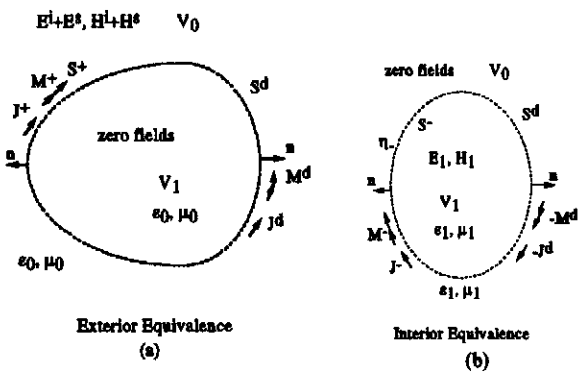

Fig.2 The equivalence problems

J^- are all axially directed and the equivalent magnetic currents M^d, M^+, and M^- are circumferentially directed. Using this fact the equivalent currents can be written in the following form:

$$J^q = J_z^q \hat{z} \quad on \; S^q \tag{1}$$

$$M^q = M_t^q \hat{t} \quad on \; S^q \tag{2}$$

where q represents $+$, $-$, or d, $\hat{z}$ is the unit vector in the z direction and $\hat{t}$ is the unit tangent. The unit tangent is defined by the equation

$$\hat{t} = \hat{z} \times \hat{n}. \tag{3}$$

In the zero field regions, the constitutive parameters are taken to be the same as in the non zero field region, so that the equivalent currents in Figs. 2a and 2b radiate into an unbounded homogeneous medium.

To formulate integral equations, the impedance boundary condition is applied on the surfaces S^- and S^+ and the continuity of the tangential components of the electric and magnetic fields on S^d is enforced. These boundary conditions are expressed as

$$E_1|_{tan} = \eta_- \eta_0 (\hat{n} \times H_1) \quad on \; S^- \tag{4}$$

$$E_0|_{tan} = \eta_+ \eta_0 (\hat{n} \times H_0) \quad on \; S^+ \tag{5}$$

$$E_1|_{tan} = E_0|_{tan} \quad on \quad S^d \tag{6}$$

and

$$\hat{n} \times H_1 = \hat{n} \times H_0 \quad on \quad S^d \quad . \tag{7}$$

The quantities η_0, η_- and η_+ are the intrinsic impedance of the free space, the normalized surface impedance on S^- and the normalized surface impedance on S^+ respectively (η_- and η_+ are normalized by η_0). Equations (4) and (5) imply that the tangential components of the electrical field can be expressed in terms of the tangential components of the magnetic field. In terms of the corresponding equivalent magnetic and electric surface currents,

$$M^+ = \eta_0\eta_+ J_z^+ \times \hat{n} = \eta_0\eta_+ J_z^+ \hat{t} \qquad (8)$$

and

$$M^- = \eta_0\eta_- J_z^- \times \hat{n} = \eta_0\eta_- J_z^- \hat{t} \qquad (9)$$

To account for different formulations, the integral tions obtained from (4) and (5) may be rewritten as follows [7]:

$$\frac{\alpha}{\eta_0} E_1|_{tan} = \beta \ \eta_- (\hat{n} \times H_1) \quad on\ S^- \qquad (10)$$

$$\frac{\alpha}{\eta_0} E_0|_{tan} = \beta \ \eta_+ (\hat{n} \times H_0) \quad on\ S^+ \qquad (11)$$

where α and β are, respectively, the combination parameters weighing the EFIE and MFIE just inside the surfaces S^+ and S^-. Thus different field formulations can be obtained by using (10) and (11), with different selections of α and β, together with (6) and (7). Equations (6) and (7) represent the PMCHW boundary condition on S^d. These formulations can be obtained according to Table I.

Table I

Generation of different formulations

	Formulation type	α	β
1.	IBCE-PMCHW	1.	0.
2.	IBCH-PMCHW	0.	-1./ηc
3.	IBCC-PMCHW	< 1.	-1./η_c
4.	IBC-PMCHW	1.	1.

In Table I, η_c stands for either η_+ or η_-. In the first two formulations, IBCE and IBCH imply that E- and H-field boundary conditions are applied, respectively, just inside the impedance surface with the implementation of the IBC approximation for the magnetic current, whereas PMCHW implies that the continuity of the tangential field components is enforced on the dielectric surface S^d. In the third formulation IBCC denotes the combination of IBCE and IBCH on the impedance surface. In the fourth formulation, IBC implies that the IBC is applied on the impedance surface. Indeed, still other formulations may be obtained when the Muller formulation is applied on S^d instead of the PMCHW formulation [8].

The currents of (1), (2), (8) and (9) give rise to TM fields only. Using this fact equations (10), (11), (6), and (7) can be reduced to scalar integral equations and written as

$$\frac{\alpha}{\eta_0}[E_{1z}(J_z^+) + \eta_-\eta_0 E_{1z}(J_z^-\hat{t}) + E_{1z}(J_z^d) + E_{1z}(M_t^d)] - \beta\eta_-[H_{1t}(J_z^-) + \eta_-\eta_0 H_{1t}(J_z^-\hat{t}) + H_{1t}(J_z^d) + H_{1t}(M_t^d)] = 0 \quad on\ S^- \qquad (12)$$

$$-\frac{\alpha}{\eta_0}[E_{0z}(J_z^+) + \eta_+\eta_0 E_{0z}(J_z^-\hat{t}) + E_{0z}(J_z^d) + E_{0z}(M_t^d)] + \beta\eta_+[H_{0t}(J_z^+) + \eta_+\eta_0 H_{0t}(J_z^+\hat{t}) + H_{0t}(J_z^d) + H_{0t}(M_t^d)] = \frac{\alpha}{\eta_0} E_z^i - \beta\eta_+ H_t^i \quad on\ S^+ \qquad (13)$$

$$\frac{1}{\eta_0}[E_{0z}(J_z^+) + \eta_+\eta_0 E_{0z}(J_z^+\hat{t}) + E_{1z}(J_z^-) + \eta_-\eta_0 E_{1z}(J_z^-\hat{t}) + E_{0z}(J_z^d) + E_{1z}(J_z^d) + E_{0z}(M_t^d) + E_{1z}(M_t^d)] = \frac{1}{\eta_0} E_z^i \quad on\ S^d \qquad (14)$$

$$H_{0t}(J_z^+) + \eta_+\eta_0 H_{0t}(J_z^+\hat{t}) + H_{1t}(J_z^-) + \eta_-\eta_0 H_{1t}(J_z^-\hat{t}) + H_{0t}(J_z^d) + H_{1t}(J_z^d) + H_{0t}(M_t^d) + H_{1t}(M_t^d) = H_t^i \quad on\ S^d \qquad (15)$$

where

$$H_t = H \cdot \hat{t} \qquad (16)$$

and

$$E_z = E \cdot \hat{z} \qquad (17)$$

The operators $E_{vz}(J)$, $E_{vz}(M)$, $H_{vt}(J)$, and $H_{vt}(M)$ are determined using the following equations:

$$E_{vz}(J_z^q) = -jk_v\eta_v \int_{S^q} J_z^q(\rho')\, g_v(\rho,\rho')\, dl \qquad (18)$$

$$E_{zi}(M_i^q) = -\hat{z} \cdot \nabla \times \int_{S^q} M_i^q(\rho')\, g_v(\rho, \rho')\, dl' \qquad (19)$$

$$H_{zi}(J_z^q) = \hat{t} \cdot \nabla \times \int_{S^q} J_z^q(\rho')\, g_v(\rho, \rho')\, dl' \qquad (20)$$

$$H_{zi}(M_i^q) = \frac{1}{jk_v\eta_v}\hat{t} \cdot \nabla \times \nabla \times \int_{S^q} M_i^q(\rho') g_v(\rho, \rho')\, dl' \qquad (21)$$

where

$$g_v(\rho, \rho') = \frac{1}{4j} H_0^{(2)}(k_v\,|\rho - \rho'|) \quad , \qquad (22)$$

$k_v = \omega\sqrt{\mu_v\epsilon_v}$, and $\eta_v = \sqrt{\mu_v/\epsilon_v}$. In the expressions above μ_v and ϵ_v are the permeability and permittivity of region V_v and $H_0^{(2)}$ is the Hankel function of second type and zero order. In Equations 18 through 21 the contour integral is evaluated on the contour that results from the intersection of S^+, S^- or S^d with the x-y plane. These contours are referred to as S^+, S^- or S^d in the context of a two-dimensional body. The contour integrals proceed in the $\hat{t}$ direction. The vector ρ is a vector in the x-y plane that identifies the field point. The vector ρ' identifies the source point.

Equations (12) to (15) are specific to the TM incident wave case. In the TE case the equivalent electric currents J^d, J^+, and J^- are all circumferentially directed and the equivalent magnetic currents M^d, M^+, and M^- are axially directed. The TE polarized case is completely dual to the TM case.

The scattered field can be calculated in the exterior equivalent situation from the currents J^+, J^d, and M^d. In equation form this is expressed as

$$E_z^s(\rho,\phi) = \eta_+\eta_0 E_z(J_z^+\hat{t}) + E_z(J_z^+) + E_z(J_z^d) + E_z(M_t^d) \qquad (23)$$

3 NUMERICAL SOLUTION

To solve the surface integral equations, the contours of the scattering body are divided into a number of linear zones. The end points of the zones lie on the actual contours of the body. The length of the zones is taken to be less than one tenth of a wavelength. The currents are expanded in pulses basis functions multiplied by to-be-determined coefficients. The point matching technique is employed to reduce the integral equations to a system of linear equations following the procedure given in [9]. Using point matching and pulses basis functions allows for accurate representation of the currents at surface of the discontinuities. Accurate representation of the currents is particularly important at the junction [10] between the dielectric surface and conducting or impedance surface. Equations (18) to (22) are reduced to a standard matrix element form and are placed in the proper location in equations (12) to (15) to obtain the moment method matrix. The solution of the matrix determines the current coefficients on all of the surfaces of the scattering body. These coefficients are then used to obtain the far scattered fields. The expressions used to calculate the matrix elements and the scattered fields are given in [9].

4 RESULTS AND DISCUSSION

The numerical solutions of the four formulations defined in Table I are verified in this section. First, circular cylindrical bodies are considered. The series solution of an impedance cylinder coated with a linear and homogeneous dielectric layer of uniform thickness is used to verify the numerical results. Fig. 3 shows the normalized bistatic scattering width (σ/λ) from an impedance cylinder of $\eta_-=0.5$ and ka=3 coated with a dielectric layer of $\epsilon_r=4.0$ and $\mu_r=1.0$, from ka=3 to kb=4. The agreement between the numerical solution of all the formulations and the series solution is satisfactory for both TM and TE polarizations. The IBCE-PMCHW and IBCH-PMCHW formulations will

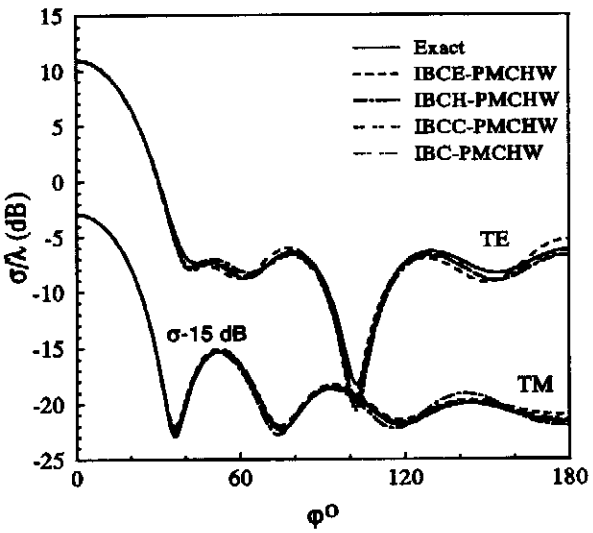

Fig. 3Bistatic scattering width of a coated impedance circular cylinder, ka=3, kb=4, $\epsilon_r=4$, $\mu_r=1$, and $\eta_-=0.5$.

fail when the impedance core is at resonance. To illustrate this failure, one specific example is presented. The case of

a circular impedance cylinder coated with a uniform dielectric layer, with ka=2.71, kb=3, ϵ_r=2, μ_r=1, and η_-

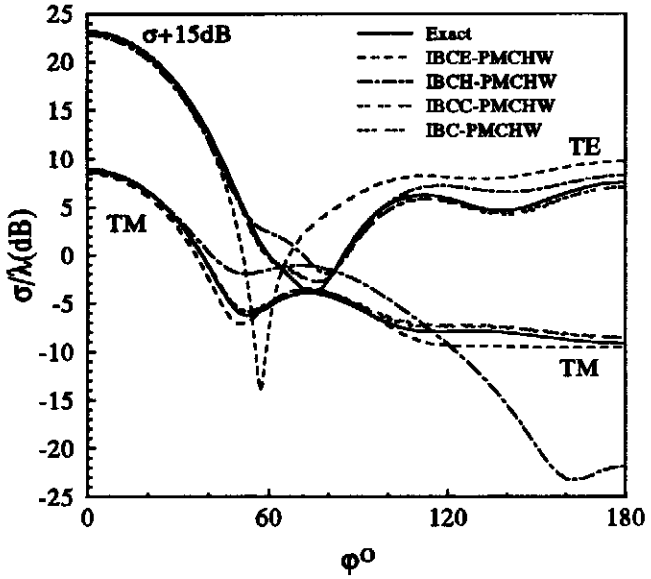

Fig. 4 Bistatic scattering width of a coated circular cylinder, ka=2.71, kb=3, ϵ_r=2, μ_r=1, and η_-=0.5.

=0.5, is considered. This example was selected because it has the same resonance frequency for both polarizations. Fig. 4 shows the comparison between the bistatic patterns computed numerically using the present method and the bistatic pattern determined using the series solution. Clearly the solution due to the IBCE-PMCHW and IBCH-PMCHW formulations fails to give the correct solution. The results from the other two formulations, the IBCC-PMCHW and IBC-PMCHW, are in good agreement with the exact solution, indicating that they are not affected by the internal resonance problem. If in the previous example the surface impedance is zero, the perfect conducting core case, the IBC-PMCHW formulation will fail to give the correct solution because it reduces to the E-PMCHW formulation.

In the previous examples we have considered completely coated objects. In the following examples we will consider partially coated objects. The bistatic scattering width of a half-dielectric/half-impedance cylinder of ka = 3, η_- = η_+ = 0.5, ϵ_r=1, and μ_r = 1 ("phantom" dielectric) is computed for all formulations. Results for the object with the "phantom" dielectric half must be the same as those for an impedance half-cylinder. In Fig. 5 a comparison is made between the numerical solution of the impedance body with the "phantom" dielectric half and the numerical solution of the impedance half-cylinder with η_+ = 0.5. Excellent agreement is observed. The same geometry is considered with ϵ_r=4 and the numerical results are compared with the numerical solution of the same object where the impedance half is replaced by a lossy dielectric half cylinder (ϵ_{r1}=8-j16

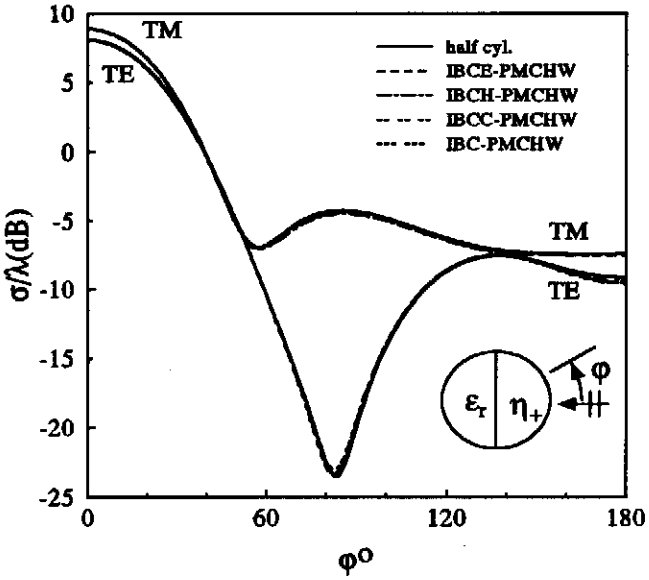

Fig. 5 Comparison between the bistatic scattering width of a half impedance cylinder and half impedance/half dielectric cylinder, ka=3, η_-=η_+=0.5,ϵ_r=1, and μ_r=1.

and μ_{r1}=2-j4), which has an equivalent normalized surface impedance of 0.5. For the lossy materials the exact boundary conditions are enforced on all the object boundaries. Fig. 6 and 7 show a comparison between the electric and magnetic surface currents, respectively, on the outer surfaces of the object using the numerical solution

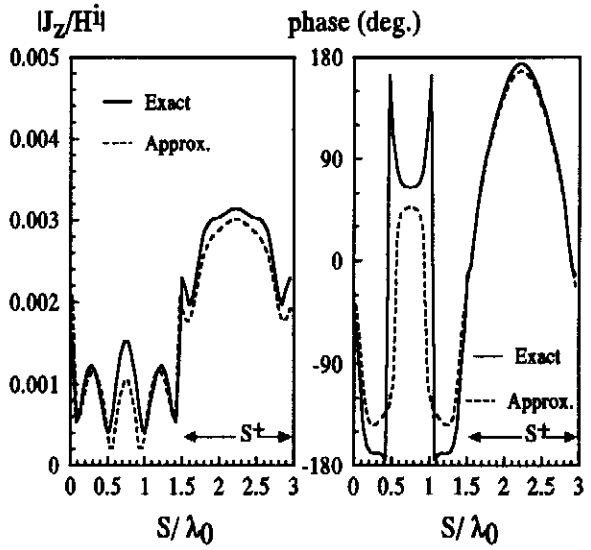

Fig. 6 (TM) Electric outer surface current on a half lossy /half dielectric cylinder and half impedance/half dielectric cylinder, ka=3, ϵ_r=4, and μ_r=1

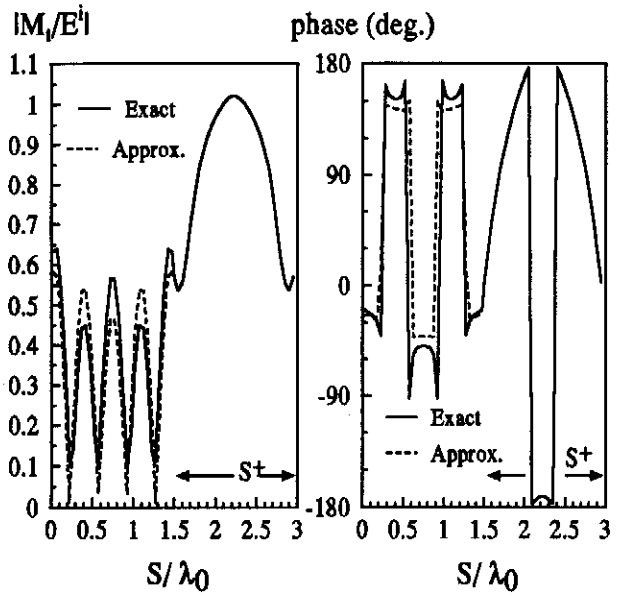

Fig. 7 (TM) Magnetic surface currents on a half lossy /half dielectric cylinder and half impedance/half dielectric cylinder, ka=3, ϵ_r=4, and μ_r=1

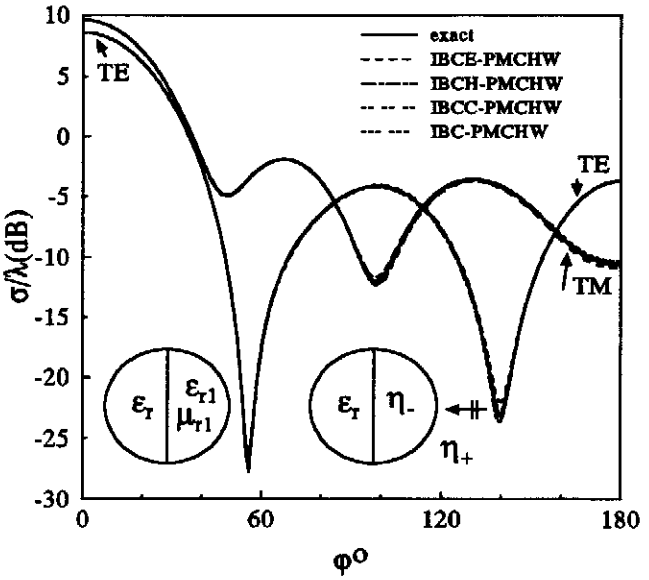

Fig. 8 Bistatic scattering width of the case in Fig. 6 and 7

with exact boundary conditions and the approximate solution of the E-PMCHW formulation for the TM polarization. Good agreement between both results is obtained in the currents magnitudes, but a large difference is observed in the phase of the electric current on the pure dielectric surface. If more accurate estimate of the surface impedance were used, better accuracy could be achieved. A significant observation is the excellent accuracy of the surface currents around the junction. The junction between three or more dielectric regions can be treated accurately even when triangle basis functions are used [10]. However, the treatments of junctions between dielectric and conductor or impedance surfaces with triangle basis functions requires an approximations which neglects the contributions due to the magnetic currents on half the triangle basis functions around the junctions. This problem does not exist when point matching and pulses basis functions are used. Fig. 8 illustrated that the exact solution and the approximate solutions for the scattering width are in excellent agreement with each other. It seems that the current error has insignificant effect on the far scattered field calculations. If the lossy material is changed so that ϵ_{r1} =6-j4 and μ_{r1}=1, the equivalent surface impedance is $\eta_- = \eta_+ = 0.3564 + j0.108$. For this example, results for the solution incorporating the exact boundary conditions and the approximate solutions (the present method) are compared in Fig. 9. The agreement in this case is not as good as in the previous example. This result is expected because the surface impedance is calculated assuming that there is no wave transmitted through the dielectric. These results indicate that the fields within the lossy material in the latter example are much larger than in the former example.

Only bistatic radar cross section has been considered to this point. The effect of different angles of incident can be investigated by computing the monostatic scattering width.

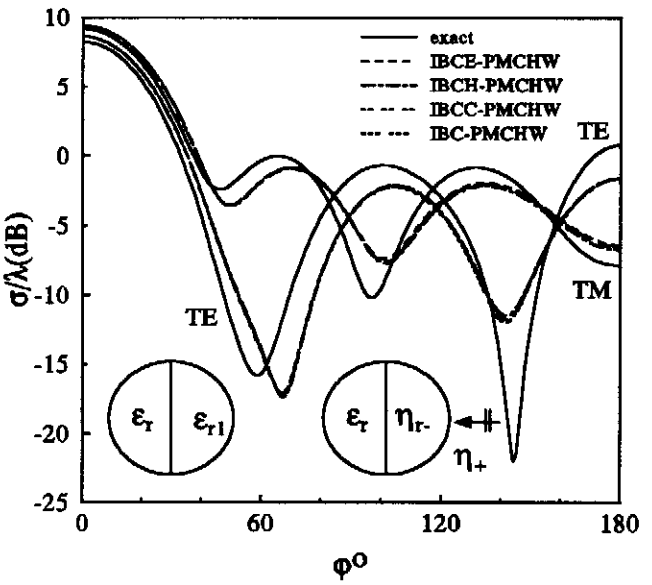

Fig. 9 Bistatic scattering width of a half lossy/half dielectric cylinder and half impedance/half dielectric cylinder, ka=3, ϵ_r=4, and μ_r=1.

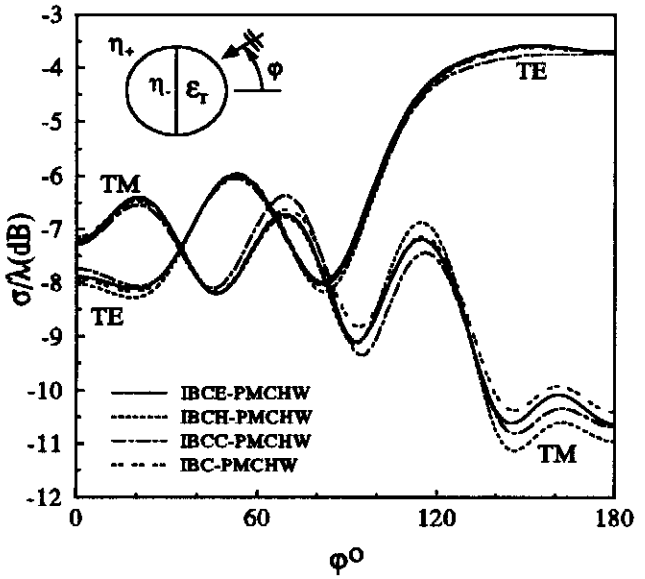

Fig. 10 Monostatic scattering width of half impedance/half dielectric cylinder, ka=3, $\eta_-=\eta_+=0.5$, $\epsilon_r=4$, and $\mu_r=1$.

The monostatic scattering width of the object considered in Fig. 8 is given in Fig. 10. The agreement between the numerical solution of the different formulations is within 0.75 dB for the TM polarization and 0.25 dB for the TE polarization.

It is known that if the surface impedance of an object equal to the intrinsic impedance of free space, the object will have zero back scattering width. This suggest that a reduction of the scattering width for an object can be obtained by manipulating the material parameters of the object. To illustrate this technique, the dielectric-coated rounded impedance cylinder shown in insert of Fig. 11a is considered. For the original scattering object, consider the core to be perfect electric conductor ($\eta_-=0.0$) coated with a uniform dielectric layer of thickness $t=0.1\lambda_0$ and $\epsilon_r=4.0$-j1.7. If the transmission line model is used to calculate the equivalent surface impedance on the outer dielectric surface, the surface impedance is $\eta_+=(0.6828+j1.0247)$ (neglecting the curvature of the surface). To reduce the scattering width, the core is selected to be an impedance surface and its surface impedance value is manipulated to make the equivalent outer surface impedance resistive and equal to the characteristic impedance of free space. It is found, using the transmission line model, that with $\eta_-=(0.092+j0.215)$ an outer surface impedance of $\eta_+=(1.0026+j0.0058)$ results. The scattering width which is calculated for the original

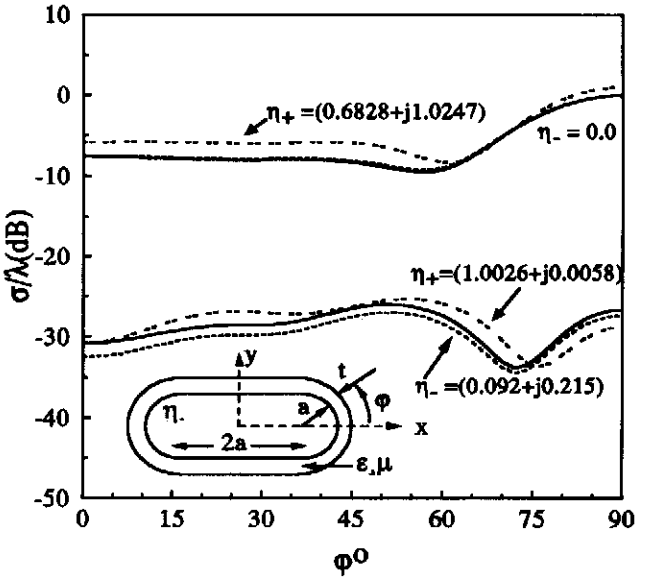

Fig. 11a Monostatic scattering width of a coated rounded impedance cylinder when $\eta_-=0$ and $\eta_-=0.092+j0.215$, $\epsilon_r=4$-j1.7, and $\mu_r=1$ (TM).

object and for the reduced scattering width body is shown in

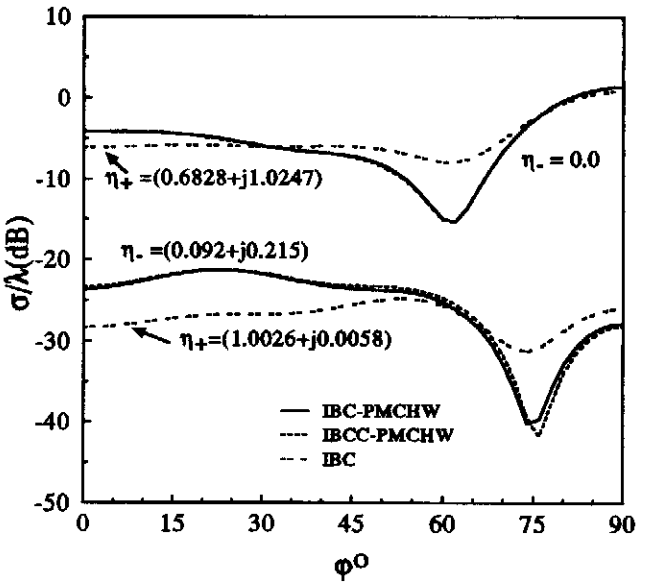

Fig. 11b Monostatic scattering width of a coated rounded impedance cylinder when $\eta_-=0$ and $\eta_-=0.092+j0.215$, $\epsilon_r=4$-j1.7, and $\mu_r=1$ (TE).

Fig. 11. In Fig 11, two models are used for each of the bodies to calculate the scattering width. The first model is the two surface model. The two surface model considers

both the inner impedance surface and the outer dielectric surface. The second model is a one surface model. The one surface model treats the outer dielectric surface as an impedance surface with equivalent surface impedance η_+. Results of the one surface model are denoted as IBC results in Fig. 11. For the body consisting of a dielectric coated core, significant reduction of the scattering width is achieved using an impedance core instead of a perfect electric conductor (PEC) core. The scattering width solution obtained using the one surface model is less accurate than that obtained using the two surface model. For the one surface model, the solution error is more pronounce in the TE case than in the TM case. This example illustrates that proper selection of the core material results in low back scattering width and that the present method can be used to accurately predict the reduced scattering width.

5 CONCLUSION

Four surface integral equation formulations are developed for two-dimensional objects composed of impedance surfaces partially coated with dielectric material. These formulations are useful in obtaining accurate and economical numerical solutions for bodies that can be modeled as coated impedance surfaces. Both TE and TM polarizations are considered. The point matching technique is used to solve the surface integral equations. The numerical solutions are verified either by comparison with the series solution for circular cylinders or by comparison with exact solutions (exact boundary conditions on all surface boundaries) for other objects. The internal resonance problem is investigated and a form of the combined field integral equation is proposed to overcome this problem. The solution accuracy is shown to be independent of the polarization. It is also shown that accurate evaluation of the surface impedance is very important to achieve good accuracy. One example is given to show that low back-scattering width can be achieved by selecting the material properties so that the outer surface impedance is equal to the characteristic impedance of free space.

6 AKNOLEDGMENTS

This work was partially supported by the National Science Foundation under Grant Number ECS-8906807.

7 REFERENCES

[1] T. B. A. Senior,"Approximate boundary conditions," *IEEE Trans. Antennas Propagat.*, vol. 29, pp. 826-829, 1981.

[2] J. R. Wait,"Use and misuse of impedance boundary conditions in electromagnetics", *Proc. PIERS Symposium*, Boston, MA, p. 358, July 1989.

[3] D.- S. Wang,"Limits and validity of the impedance boundary condition for penetrable surfaces", *IEEE Trans. Antennas Propagat.*, Vol. AP-35, pp. 453-457, No. 4, 1987.

[4] S.- W. Lee,"How good is the impedance boundary condition?", *IEEE Trans. Antennas Propagat.*, Vol. AP-35, pp. 1313-1315, No. 11, 1987.

[5] J. L. Volakis and T. B. A. Senior,"Application of a class of generalized boundary conditions to scattering by a metal-backed dielectric half-plane," *Proc. IEEE*, Vol. 77, pp. 796-805, May 1989.

[6] T. B. A. Senior and J. L. Volakis,"Derivation and application of a class of generalized boundary conditions," *IEEE Trans. Antennas Propagat.*, Vol. AP-37, pp. 1566-1572, No. 12, 1989.

[7] A. A. Kishk,"Electromagnetic scattering from composite objects using a mixture of exact and impedance boundary conditions," *IEEE Trans. Antennas Propagat.*, Vol. AP-39, pp. 826-833, No. 6, 1991.

[8] A. A. Kishk and L. Shafai,"On the accuracy limits of different integral-equation formulations for numerical solution of dielectric bodies of revolution," *Canadian Journal of Physics*, vol. 63, no. 12, pp. 1532-1539, 1985.

[9] P. M. Goggans, "A combined method-of-moments and approximate boundary condition solution for scattering from a conducting body with a dielectric-filled cavity," *Ph.D. Dissertation*, Auburn University, 1990.

[10] J. M. Putnam and L. N. Medgyesi-Mitschang,"Combined field integral equation formulation for inhomogeneous two- and three-dimensional bodies: The junction problem,"*IEEE Trans. Antennas Propagat.*, Vol. AP-39, pp. 667-672, No. 5, 1991.